Synthesizing Cell Protein data for Human Protein Cell Profiling Using Dual Deep Generative Modeling

Rakesh Ranjan
Graduate School of Life Science and Systems Engineering
Kyushu Institute of Technology
Kitakyushu City, Fukuoka, Japan
sweetatyagiaz@gmail.com

Sozo Inoue
Graduate School of Life Science and Systems Engineering
Kyushu Institute of Technology
Kitakyushu City, Fukuoka, Japan
sozo@brain.kyutech.ac.jp

Tomohiro Shibata
Graduate School of Life Science and Systems Engineering
Kyushu Institute of Technology
Kitakyushu City, Fukuoka, Japan
tom@brain.kyutech.ac.jp

***Abstract*—To understand the biology of health, and how molecular dysfunction leads to disease, knowledge of the human cell is essential. The protein is the core unit of the human body made from trillions of cells, forming the body's various tissues. These tissues come together to create human organs. It is essential to understand the Spatio-temporal distribution of proteins in cells and to investigate human RNA-sequencing for human genes characterization. For this, it requires a massive amount of annotated data. However, due to many considerations like the high cost of data sample collection, lack of data sample availability, and lawful clauses for patient privacy, the majority of medical data is out of reach for general public research. In this study, we propose a new dual deep generative method for synthesizing human cell protein images by using the Generative Adversarial Network technique. Specifically, for that, we pair original cell protein images with their respective Cell-protein-tree. These pairs are then used to learn the mapping from a binary cell protein to a new cell protein image. For this purpose, we use an image-to-image translation technique based on adversarial learning. The generated cell protein images are expected to preserve the structural and visual quality of the training images. Visual and quantitative analysis of the experimental results demonstrates that the synthesized data are preserving the desired quality while maintaining the different forms of original data.**

***Contribution*—We have proposed a new dual deep generative model for synthesizing cell protein data.**

***Keywords*—Dual deep generative modeling, Cell protein image synthesis, Image-to-image translation, Generative adversarial network**

I. Introduction

Resolving the molecular details of proteome variation at a subcellular level in the different tissues and organs of the human body would revolutionize how doctors and researchers understand, diagnose, and treat disease. This can only be achieved by studying the molecular components of its smallest functional unit, the cell, which is internally organized into compartments called organelles. The spatial partitioning provided by organelles creates an enclosed environment for chemical reactions tailored to fulfill specific functions. These functions are tightly linked to a particular set of proteins. Therefore, resolving the human proteome's subcellular location provides information about the role of the organelle and its underlying cellular mechanisms. By analyzing protein expression data for both healthy and disease tissues [1], on many different individual patients to evaluate the heterogeneity of tissue profiles [2][3].

With the advancements of machine learning techniques, especially deep learning techniques, in medical technology, have tremendously increased the requirement of annotated medical data. These medial data contain a rich set of information that has a strong potential to improve medical research and developments. The wide availability and open access of annotated medical data may allow the research community to develop and validate new sophisticated techniques and to explore new research field which can spark exponential growth in the medical industry. However, these techniques require a considerable amount of annotated data for model training and its validation. But data collection is not only a complex but also very costly. It requires an enormous amount of capital and experts to validate and annotate it. Apart from that, especially in medical data, the complexity, like the legal formality of data sharing, increases as data privacy is a significant concern. These complex requirements slow or even prevent data sharing between researchers in all but the closest collaborations. Therefore, the problem of data generation has been greatly focused in recent years.

In recent years, with the advancement of machine learning techniques, the data-driven approach for synthesizing real-world data has emerged as one of the favorite topics in the research community. In this context, with the help of machine learning recent techniques, the system is able to extract the inherent variability from the large pool of training data. Ideally, the model can learn the intrinsic probability distribution, which uniquely defines the dataset. Once trained, the system can sample out as many as new synthetic data that are likely to lie with the same probability distribution as the original dataset. This approach has been successfully applied to solve various problems of many different areas like to improve classification error of multi-sequence Magnetic resonance imaging (MRI) [4], also used to estimate cross-modality transformation [5] or to perform knowledge transfer by learning feature map.

In this study, we proposed a new machine learning-based method for synthesizing cell protein images data by learning an inherent nonlinear mapping from the source dataset to the synthetic target dataset. For this, we have used a famous data-driven adversarial framework, generative adversarial network (GAN) [7], for generating more realistic synthetic cell protein data.

In this work, we proposed a dual generative method, by using the generative adversarial network [7] with its variants, for learning non-linearity and structural dependency to produce photorealistic cell protein images. Our proposed method is comprised of two different GANs, by breaking down the whole problem into two parts: Stage-I GAN and Stage-II GAN. Stage-I GAN produces the Cell-protein-tree masks that represent the variable geometries of the original

978-1-7281-9331-1/20/$31.00 ©2020 IEEE

Cell Protein dataset. Whereas Stage-II GAN, translate the produced cell-protein-tree masks, generated by Stage-I GAN, to the photorealistic cell protein images, while preserving the texture and structural information into the images.

The rest of the paper is organized as follows: Related works are presented in Section II, followed by Section III, which contains the detail about the proposed methodology and model evaluation. The datasets used in experiments are also discussed in this section. The experimental results and discussion presented in Section IV and conclusions and future woke presented in Section V.

II. Related Works

A. Medical Image Synthesis

Synthesizing medical image data has been gaining popularity in the recent decade due to clinical importance and data privacy. The ability to generate high-quality of synthetic medical data in volume will provide great help to the research community.

In recent years several machine learning data-driven techniques has been developed for synthesizing medical data. Traditional synthesis method like patch-based regression tasks [14], which use the image patch from source image for predicting into the target image. Besides the patch-based regression model, the sparse representation method has also gained popularity for medical image synthesis for solving the problem of super-resolution (SR) and cross-modality by proposing supervised convolutional sparse coding [15] method. Atlas-based model [16] is another popular method for medical image synthesis. This method translates atlas-to-image from the source modality by adopting the paired image atlases. More recently, a data-driven approach from a deep learning-based GAN framework is considered one of the most popular methods for synthesizing medical images, such as retinal images [17], CT images [18], ultrasound images [19], MR images [20] and so on. For example, [17] utilized a retinal vessel tree to synthesizing corresponding fundus images. For synthesizing computed tomography (CT) images, Nie et al. [18] used a context-aware GAN method with MR images data. Wolternik et al. [22] used GAN to transform low-dose CT into routine-dose CT images. Wang et al. [21] also present a promising result to estimate high-dose PET images from low-dose ones by utilizing the powerful capacity of the GAN method. There is very limited research available on cell protein synthesis. A bit similar to our work, Anton et al. [23] proposed a star-shaped GAN model to synthesize cell images by fluorescence microscopy. But the generated image quality is low, as they have used single GAN network architecture, even though they have considered lower-dimensional image data.

B. Image-to-image translation

In the field of medical imaging, the texture of the image contains very useful information. The loss of texture information from the image is considered a massive loss of information. For this reason, image-to-image translation is considered one of the most important forms of the GAN method for medical image synthesis. In 2016, a special type of GAN framework, Patch GAN or pix2pix GAN [25], has been introduced for supervised image-to-image translation problems. The generator network receives a grayscale image from the input domain as input. It is translated to the color image as a target domain by minimizing the adversarial loss and pixel reconstruction error. Afterward, several modifications have been proposed to minimize the adversarial loss and reconstruction loss to preserve the quality of the generated image. Like PAN [26], feature matching loss in place of the pixel loss introduced to minimize the texture loss of generated images. FilasGAN [27] proposed one-to-many translation using a pre-trained network to transfer the texture information of source data to the target data by considering style loss. In a similar context, the conditional GAN [11] introduced for capturing the source data texture information by learning the translation mapping over conditional constraint. Moreover, several unsupervised variants of the GAN network were introduced, such as CycleGAN [24] and DiscoGANs [28], where training did not require pair image data. For generalizing the conditional GAN, CycleGAN [24] was proposed with an unsupervised variant feature.

Recently in the field of medical imaging, GAN has been getting more attention. To translate the MR to CT image D. Nie [29] uses the pix2pix network architecture, where they used gradient-based loss function for minimizing reconstruction error. For compressed sensing (CS) MRI reconstruction [6] also used image-to-image translation, which used Wasserstein distance loss and a pretrained network for feature matching losses. For synthesizing retinal images, [17] also used a pix2pix network by combining adversarial loss with global $L1$ loss.

III. Methods

As medical image contains very high structural and texture information, while synthesizing the medical data, it is essential to preserve this information. The lack of these essential textural and structural information in synthetic data is unacceptable for medical standards. Due to the vanishing gradient problem in GAN, when the image data dimension increases, a single GAN network is not able to preserve all these pieces of information. For keeping this in mind, we have proposed a dual deep generative network structure, where first network, Stage-I GAN, focus only on generating unique cell-protein-tree geometrics from the lower dimension problem. At the same time, this allows the second network, Stage-II GAN, only to generate the texture, color, and lighting information. By breaking down the problem into two sub-problems, we overcame the problem of standard GAN for generating high-dimensional image data.

Since the inception of the GAN network, proposed by Goodfellow [7], the framework has significantly attracted the attention of the research community. This framework is comprised of two networks, one is called generator network G, and second is discriminator network D. G is a generator network which generates the data from the normal distribution. Whereas D is a binary classifier, which classifies the data generated by G is from the training set (original set) or not (synthetic set). For this, both networks trained jointly and tried to minimize their respective loss function by progressively learning from the network loss and trying to generate a more realistic synthetic sample that can deceive D. G minimizes its loss function by producing sample that D will classify it as real, called adversarial loss. Both networks jointly try to optimize the objective function $V(D,G)$ modeled as:

$$\min_G \max_D V(D,G) = \mathbb{E}_{x\sim p_{data}}[\log D\,(x)] + \\ + \mathbb{E}_{x\sim p_z}\left[\log\left(1 - D\big(G(z)\big)\right)\right] \quad (1)$$

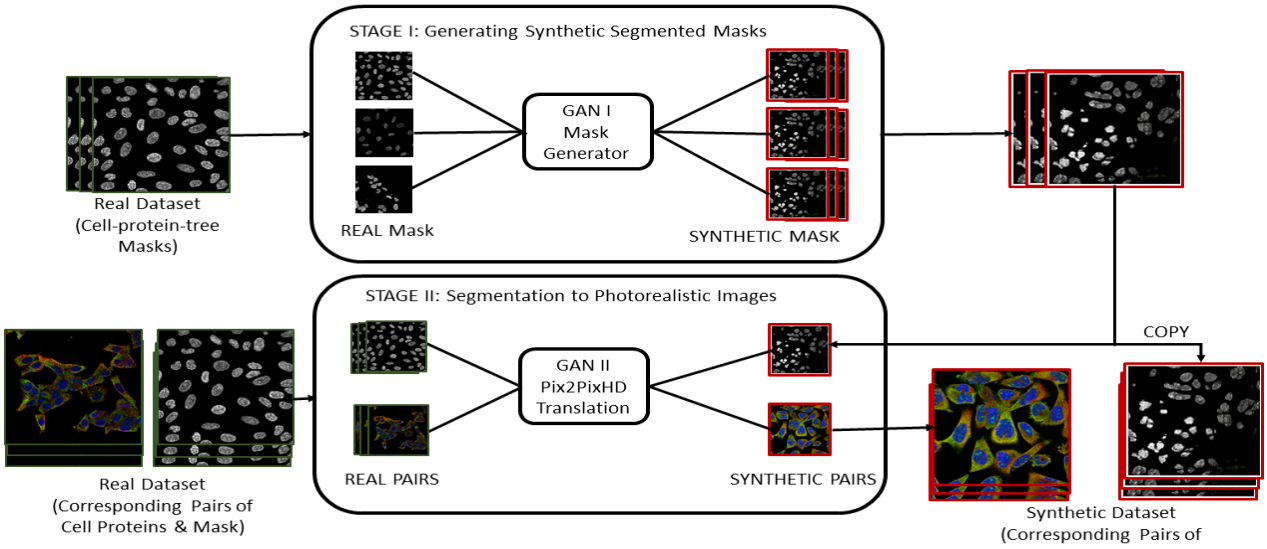

Fig. 1 Flowchart of proposed method pipeline.

where x is a sample drawn from the original data distribution p_{data} and z is a sample from the noise distribution p_z, generally from normal distribution. G always wants a small value of the objective function $V(D,G)$, where D wants larger value.

A. *Stage-I GAN*

Stage-I GAN objective is to learn the structural mapping from original data and to generate Cell-protein-tree masks. The network structure of Stage-I GAN is based on the architecture of deep convolutional generative adversarial network (DCGAN) [8] network.

This network has demonstrated competitive results while simultaneously improving training stability in compression to standard GAN. In comparison with another generative model, DCGAN has an important feature that it is fully convolutional. In DCGAN, convolutional layers were used in place of pooling layers to preserve the important features found in medical images.

$$l_D = \frac{1}{m}\sum_{i=1}^{m}\left[log\left(D\left(G(z^i)\right)\right) + log\left(1 - D(x^i)\right)\right] \quad (2)$$

where G and D are generator and discriminator networks, respectively. z is the input noise vector from normal distribution, and m is the mini-batch size. x is the image from real sample, and i is the index of the image from original data samples. For generating synthetic image samples, the network G is initialized with noise vector from the normal distribution. The cross-entropy loss function has been used to train the discriminator network D. The generator loss function is:

$$l_G = \frac{1}{m}\sum_{i=1}^{m} log\left(1 - D(x^i)\right) \quad (3)$$

The network D and G always try to minimize their respective loss function competitively as both networks are trained jointly.

B. *Stage-II GAN*

Stage-II GAN objective is to translate Cell-protein-tree mask to corresponding photorealistic cell protein image, based on pix2pix GAN network [9]. This is also called conditional generative adversarial network (CGAN). Its objective to condition the two network G and D to a vector y and input image X that represents the mapping between the segmentation protein mask and photorealistic image. CGAN can also be modeled similar to the regular GAN by this function, with an additional input parameter y:

$$\min_G \max_F V(D,G) = \mathbb{E}_{p_{data}}[logD(x,y)] + \\ + \mathbb{E}_{z-p_z}\left[log\left(1 - D\big(G(z,y)\big)\right), y\right] \quad (4)$$

In doer to find a mapping for image-to-image translation, the Stage-II GAN network is trained with a cell-protein-tree mask with its respective real cell protein image dataset. After the training model will able to translate the given geometry to a photorealistic image with the input of a given cell-protein-tree mask.

C. *Dataset*

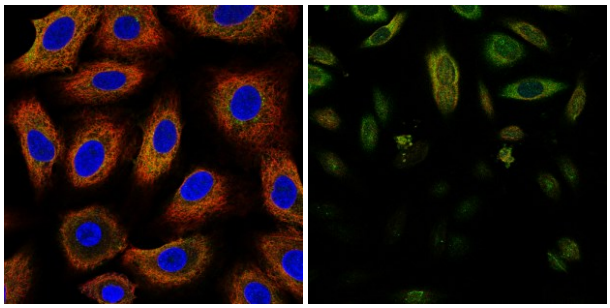

Fig. 2 Example Cell Protein images of HPA dataset used for training.

We used HPA (Human Protein Atlas) dataset [30], proposed in 2003, for mapping all protein types in cells, tissues, and organs, using anti-body labels with microscopy. For systematic analysis of image-based map for the detailed spatial distribution of proteins in human cell. The Cell Atlas in the HPA is building a proteome scale map of protein

subcellular localization via hundreds of high-resolution confocal immunofluorescence images.

The HPA dataset provides high-resolution insights into the expression and Spatio-temporal distribution of proteins within human cells. The mRNA expression of all human genes is characterized by deep RNA-sequencing, which uses a panel of 64 cell lines to represent various cell populations in different organs and tissues of the human body. Based on corresponding gene expression, the subcellular distribution of each protein is investigated. The protein localization data is derived from antibody-based profiling by immunofluorescence confocal microscopy and classified into 32 different organelles and fine subcellular structures. In March 2010, the 6th version of HPA launched, which contained 11,274 antibodies corresponding to 8,489 protein-coding genes.

D. Model Evaluation

In the case of machine learning-based generative modeling, which works on the principle of adversarial learning of data distribution, it is crucial to verify that model has not memorized merely the distribution of the training dataset. This can be accomplished by analyzing the distance between the synthetic dataset and the training dataset. If the model has not memorized the distribution, it is expected that there will be some visual difference between the training set and the synthetic set, generated by the model. In GANs, KL-divergence is considered one of the standard scores to measure the difference between the distributions of two datasets. The KL-divergence score, which used to calculate the correlation between the generated dataset and the original dataset, is calculated by:

$$KL(P,Q) = \sum_i P_i \left(ln \frac{P_i}{Q_i} \right) \quad (5)$$

Mutual information (MI) only considers the intensity statistical characteristics of an image to understand the pixel intensity distribution by histogram visualization. Due to this, MI is considered one of the most popular similarity measures used for image visual difference evaluation and medical image registration [12]. MI in case of image matching, does not require the signal to be the same in two images. It is a measure of how well it can predict the signal in the referenced image by given the signal intensity in the observed image. MI between two images is calculated from:

$$MI(d,d') = \sum_{d_i \in d} \sum_{d_i' \in d'} p(d_i, d_i') log \left(\frac{p(d_i,d_i')}{p(d_i)p(d_i')} \right) \quad (6)$$

where d_i, d_i' respectively are pixel intensities in the real image and synthetic image, $p(d_i)$ and $p(d_i')$ respectively denote the one-dimensional probability density functions of the images d_i and d_i' and $p(d,d')$ is the two-dimensional joint probability density function, where MI is a metric from the joint (2D) histogram. When the signal is highly concentrated in a few bins, the metric value is high, but when the signal is spared across many bins the value is low.

Several methods exist for quantitatively evaluating image structural similarity, out of which Structural Similarity (SSIM) [13] score is considered as one of the most important and widely used for GANs evaluation. For structural quality evaluation of generated images, we have applied SSIM Index, widely used for structural similarity measurement between two images. It is valued between -1 to 1. The SSIM measure between two image x and y is:

$$SSIM(x,y) = \frac{(2\mu_x\mu_y + c_1)(2\sigma_{xy} + c_2)}{(\mu_x^2 + \mu_y^2 + c_1)(\sigma_x^2 + \sigma_x^2 + c_2)} \quad (7)$$

In practice, it is essential to measure the overall quality of an image. For this, we have calculated a mean SSIM (MSSIM) index, as the model is initializing from the normal distribution, evaluating the overall performance of our proposed network.

$$MSSIM = \frac{1}{M} \sum_{j=1}^{M} \max SSIM \left(x_j, y_1^K \right) \quad (8)$$

where x is the random synthetic generated image and y is the corresponding referenced image from real dataset with highest SSIM index; M represent the count of generated samples used for evaluation; and K is the count of real dataset sample.

Lastly, to evaluate our proposed pipeline method, we have trained a standard GAN for baseline compression. For visual and structural quality evaluation, we have calculated the statistical score, which is considered a standard score to evaluate generative modeling, like KL-divergence score and Structural Similarity Score (SSIM). We also use the MI score for evaluating visual quality of the synthetic dataset.

IV. RESULTS AND DISCUSSIONS

This section first describes the model architecture and their hyper-parameters setting for training; secondly, we have demonstrated the detailed investigation of the proposed pipelined method and statistical evaluation metrics and comparison with standard GAN as a baseline model.

We have used Keras and Tensorflow Library for implementing the proposed network. In both network Stage-I GAN and Stage-II GAN, we are using DCGAN as network configuration. The generator G takes input Z = 100 as random noise from the normal distribution. The network weights parameters, θ, β of both G and D, is initialized with [-0.05, 0.05] truncated normal distribution of zero-mean, and 0.025 of standard deviation (SD). The weight θ of G is updated using Adam optimizer [31] with learning rate of 0.00015, while the vanilla stochastic gradient descent updates β of D with learning rate of 0.0002. In both G and D at each convolution (or transpose convolution) layer (5, 5) kernel size and (2, 2) stride is used. A batch normalization layer is used after each convolution (or transpose convolution) layer. ReLU and Leaky ReLU are used as the activation function in G and D with α=0.2, respectively.

TABLE I. KL-DIVERGENCE SCORE

Method	***Synthetic***	***Real***
Standard GAN	38.276	3.1517×10^{-5}
Proposed Method	3.794	3.1517×10^{-5}

To examine the overall performance of our method, we obtained the variance between the synthetic and real datasets through a Kullback-Leibler (KL) divergence score, to show the difference between the distribution of two datasets.

Table I, present the KL-divergence score of the proposed method and standard GAN. The synthetic data score from comparing the synthetic and real dataset is 3.794 for the proposed method, and 38.276 is for standard GAN, while the real data score is 3.1517×10^{-5}, measured by comparing two random subsets from the real dataset. The KL-divergence score of the real dataset is low, as the both image subsets are from the same dataset. The higher KL-divergence score of the synthetic dataset implies that our proposed network has not merely copy the original distribution. Whereas the KL-divergence score of standard GAN is very high, which states that the network is not able to produce the structural and visual quality as compared to the real dataset.

For visual quality evaluation of synthetic dataset generated by our proposed method, we have calculated mutual information value by using equation 6, where MI is used as metric for closeness between two images. We have calculated mean MI score over 100 random images generated by our proposed method and standard GAN. For this we select an image d' from synthetic dataset and find the closest match d in in training dataset for every image and so on.

TABLE II. MUTUAL INFORMATION METRIC

Method	***Mean MI***
Standard GAN	0.675
Proposed Method	0.932

TABLE III. MEAN STRUCTURAL SIMILARITY (SSIM) INDEX

Method	***Mean SSIM***
Standard GAN	0.629
Proposed Method	0.899

From Table II, the mean MI score of standard GAN is 0.675, which can also be observed from the Fig. 3 (a) as image visual quality is bit blurred, is lower as image pixels are less concentrated into a small number of bins. Whereas the MI score of proposed method is 0.932, much higher than standard GAN, which state that our Stage-II GAN network, which is responsible to perform image-to-image translation, is synthesizing better visual quality or texture information than standard GAN.

It is worth noting that as Stage-II GAN, is able to translate higher texture information into synthetic image. Due to this the signal in the synthetic image, is more concentrated into a small number of bins and hence MI score, between proposed method synthetic dataset and original dataset, is higher. In Fig. 4 we show random samples gallery of synthetically generated cell protein images and their corresponding cell-protein-tree masks.

Fig. 5 shows the sample output of the cell protein image, generated by our proposed method, with the closest referenced image from the original dataset. We have calculated the MSSIM index for the proposed method and the standard GAN model over 100, $M = 100$, random images as a whole. As in both methods, the network is initializing from the normal distribution, we have considered the highest SSIM index value between synthetic image and corresponding referenced image from the real dataset.

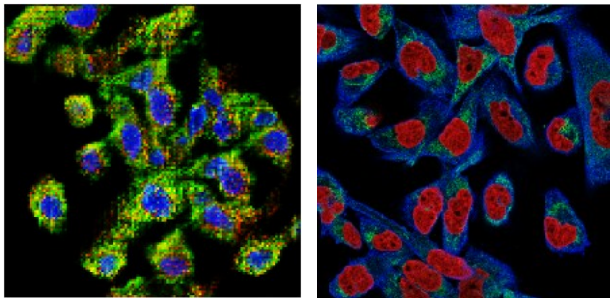

Fig. 3 (a) generated by standard GAN, (b) generated by proposed pipelined method. It clearly shows that standers GAN is not able to preserve the texture and structural quality. While the image generated by the proposed pipelined method is able to preserve the quality.

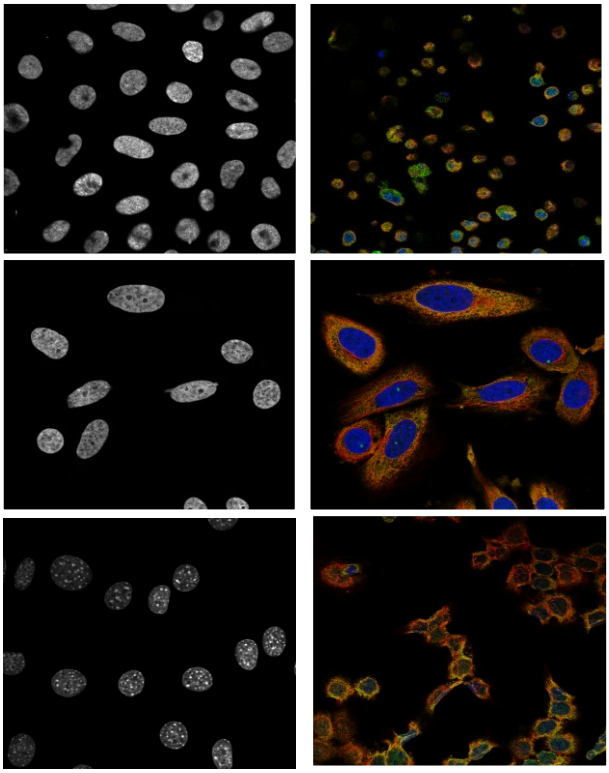

Fig. 4 Random samples gallery of cell-protein-tree masks and corresponding cell protein images generated by our proposed model.

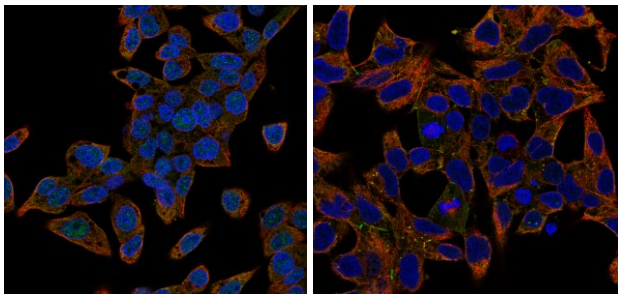

Fig. 5 Cell protein image (right) generated by proposed method with closest real image (left).

The MSSIM score of the proposed method is 0.899, which states approx. 90% similarity between original dataset and synthetic dataset produced by the proposed model. Whereas the MSSIM score of the standard GAN is 0.629, which is below the threshold, this is because the standard GAN

network is not able to preserve the structural and visual quality. From Table III, it can be observed that the standard GAN model is not able to preserve the image quality whereas the proposed method is able to synthesize image with high SSIM index.

V. Conclusion and Future work

In this work, we have presented a dual deep generative model approach for synthesizing new cell-protein-tree masks and corresponding photorealistic cell protein images. Our proposed model learns the underlying distribution of plausible cell protein images from the dataset of pair of cell-protein-tree and cell protein images. Specifically, we used a dual generative approach for synthesizing photorealistic cell protein images. Once trained, it can generate both cell-protein-tree masks and cell protein images that contain rich geometric structure and visual information. The resulting model shows a 90% of MSSIM score, which state that synthesized images contain high structural information. The mean MI score of 0.932 shows that method is producing rich visual quality image. Furthermore, the KL-divergence score of synthetic datasets is higher than the real dataset shows that the proposed method is simply not copy the original distribution.

Future works include having the model to synthesize high dimensional cell protein image data with rich visual and structural information. Furthermore, a single unified network structure for synthesizing high dimensional medical image needs to develop.

References

[1] Uhlen, M., & Ponten, F. (2005). Antibody-based Proteomics for Human Tissue Profiling. *Molecular & Cellular Proteomics, 4*(4), 384-393. doi:10.1074/mcp.r500009-mcp200.

[2] Kononen, J., et al. (1998). Tissue microarrays for high-throughput molecular profiling of tumor specimens. *Nature Medicine, 4*(7), 844-847. doi:10.1038/nm0798-844.

[3] Hewitt, S. M. (n.d.). Design, Construction, and Use of Tissue Microarrays. *Protein Arrays,* 061-072. doi:10.1385/1-59259-759-9:061.

[4] Ledig, C., et al. (2017). Photo-Realistic Single Image Super-Resolution Using a Generative Adversarial Network. *2017 IEEE Conference on Computer Vision and Pattern Recognition (CVPR)*. doi:10.1109/cvpr.2017.19.

[5] Gauthier, J. (2014). Conditional generative adversarial nets for convolutional ... Retrieved August 15, 2020, from https://www.foldl.me/uploads/2015/conditional-gans-face-generation/paper.pdf.

[6] Quan, T. M., Nguyen-Duc, T., & Jeong, W. (2018). Compressed Sensing MRI Reconstruction Using a Generative Adversarial Network With a Cyclic Loss. *IEEE Transactions on Medical Imaging, 37*(6), 1488-1497. doi:10.1109/tmi.2018.2820120.

[7] Goodfellow, I.J., et al. (2014). Generative Adversarial Nets. Retrieved August 15, 2020, from https://papers.nips.cc/paper/5423-generative-adversarial-nets.pdf.

[8] Radford, A., Metz, L., & Chintala, S. (2016, January 07). Unsupervised Representation Learning with Deep Convolutional Generative Adversarial Networks. Retrieved August 15, 2020, from https://arxiv.org/abs/1511.06434.

[9] Wang, T., Liu, M., Zhu, J., Tao, A., Kautz, J., & Catanzaro, B. (2018). High-Resolution Image Synthesis and Semantic Manipulation with Conditional GANs. *2018 IEEE/CVF Conference on Computer Vision and Pattern Recognition*. doi:10.1109/cvpr.2018.00917.

[10] Mogren, O. (2016, November 29). C-RNN-GAN: Continuous recurrent neural networks with adversarial training. Retrieved August 15, 2020, from https://arxiv.org/abs/1611.09904.

[11] Mirza, M., & Osindero, S. (2014, November 06). Conditional Generative Adversarial Nets. Retrieved August 15, 2020, from https://arxiv.org/abs/1411.1784.

[12] Pluim, J., Maintz, J., & Viergever, M. (2003). Mutual-information-based registration of medical images: A survey. *IEEE Transactions on Medical Imaging, 22*(8), 986-1004. doi:10.1109/tmi.2003.815867.

[13] Wang, Z., Bovik, A., Sheikh, H., & Simoncelli, E. (2004). Image Quality Assessment: From Error Visibility to Structural Similarity. *IEEE Transactions on Image Processing, 13*(4), 600-612. doi:10.1109/tip.2003.819861.

[14] Torrado-Carvajal, A., et al. (2015). Fast Patch-Based Pseudo-CT Synthesis from T1-Weighted MR Images for PET/MR Attenuation Correction in Brain Studies. *Journal of Nuclear Medicine, 57*(1), 136-143. doi:10.2967/jnumed.115.156299.

[15] Huang, Y., Shao, L., & Frangi, A. F. (2017). Simultaneous Super-Resolution and Cross-Modality Synthesis of 3D Medical Images Using Weakly-Supervised Joint Convolutional Sparse Coding. *2017 IEEE Conference on Computer Vision and Pattern Recognition (CVPR)*. doi:10.1109/cvpr.2017.613.

[16] Roy, S., Carass, A., & Prince, J. L. (2013). Magnetic Resonance Image Example-Based Contrast Synthesis. *IEEE Transactions on Medical Imaging, 32*(12), 2348-2363. doi:10.1109/tmi.2013.2282126.

[17] Costa, P., et al. (2018). End-to-End Adversarial Retinal Image Synthesis. *IEEE Transactions on Medical Imaging, 37*(3), 781-791. doi:10.1109/tmi.2017.2759102.

[18] Nie, D., et al. (2018). Medical Image Synthesis with Deep Convolutional Adversarial Networks. *IEEE Transactions on Biomedical Engineering, 65*(12), 2720-2730. doi:10.1109/tbme.2018.2814538.

[19] Tom, F., & Sheet, D. (2018). Simulating patho-realistic ultrasound images using deep generative networks with adversarial learning. *2018 IEEE 15th International Symposium on Biomedical Imaging (ISBI 2018)*. doi:10.1109/isbi.2018.8363780.

[20] Dar, S. U., Yurt, M., Karacan, L., Erdem, A., Erdem, E., & Cukur, T. (2019). Image Synthesis in Multi-Contrast MRI With Conditional Generative Adversarial Networks. *IEEE Transactions on Medical Imaging, 38*(10), 2375-2388. doi:10.1109/tmi.2019.2901750.

[21] Wang, Y., et al. (2019). 3D Auto-Context-Based Locality Adaptive Multi-Modality GANs for PET Synthesis. *IEEE Transactions on Medical Imaging, 38*(6), 1328-1339. doi:10.1109/tmi.2018.2884053.

[22] Wolterink, J. M., Leiner, T., Viergever, M. A., & Isgum, I. (2017). Generative Adversarial Networks for Noise Reduction in Low-Dose CT. *IEEE Transactions on Medical Imaging, 36*(12), 2536-2545. doi:10.1109/tmi.2017.2708987.

[23] Osokin, A., Chessel, A., Salas, R. E., & Vaggi, F. (2017). GANs for Biological Image Synthesis. *2017 IEEE International Conference on Computer Vision (ICCV)*. doi:10.1109/iccv.2017.245.

[24] Zhu, J., Park, T., Isola, P., & Efros, A. A. (2017). Unpaired Image-to-Image Translation Using Cycle-Consistent Adversarial Networks. *2017 IEEE International Conference on Computer Vision (ICCV)*. doi:10.1109/iccv.2017.244.

[25] Isola, P., Zhu, J., Zhou, T., & Efros, A. A. (2017). Image-to-Image Translation with Conditional Adversarial Networks. *2017 IEEE Conference on Computer Vision and Pattern Recognition (CVPR)*. doi:10.1109/cvpr.2017.632.

[26] Wang, C., Xu, C., Wang, C., & Tao, D. (2018). Perceptual Adversarial Networks for Image-to-Image Transformation. *IEEE Transactions on Image Processing, 27*(8), 4066-4079. doi:10.1109/tip.2018.2836316.

[27] Zhao, H., Li, H., & Cheng, L. (2017, June 07). Synthesizing Filamentary Structured Images with GANs. Retrieved August 15, 2020, from https://arxiv.org/abs/1706.02185.

[28] Kim, T., Cha, M., Kim, H., Lee, J., & Kim, J. (2017, May 15). Learning to Discover Cross-Domain Relations with Generative Adversarial Networks. Retrieved August 15, 2020, from https://arxiv.org/abs/1703.05192.

[29] Nie, D., et al. (2018). Medical Image Synthesis with Deep Convolutional Adversarial Networks. *IEEE Transactions on Biomedical Engineering, 65*(12), 2720-2730. doi:10.1109/tbme.2018.2814538.

[30] Thul, P., et al. (2017, May 26). A subcellular map of the human proteome. Retrieved August 15, 2020, from https://science.sciencemag.org/content/356/6340/eaal3321.full.